Synthesis and Characterization of Melt-Processable Polyimides Derived from 1,4-Bis(4-amino-2-trifluoromethylphenoxy)benzene

H. J. Zuo, J. S. Chen, H. X. Yang, A. J. Hu, L. Fan, S. Y. Yang

Laboratory of Advanced Polymer Materials, Institute of Chemistry, Chinese Academy of Sciences, Zhongguancun, Beijing 100080, China

Received 20 February 2007; accepted 4 June 2007
DOI 10.1002/app.26965
Published online 25 September 2007 in Wiley InterScience (www.interscience.wiley.com).

ABSTRACT: A series of molecular-weight-controlled imide resins end-capped with phenylethynyl groups were prepared through the polycondensation of a mixture of 1,4-bis(4-amino-2-trifluoromethylphenoxy)benzene and 1,3-bis(4-aminophenoxy)benzene with 4,4′-oxydiphthalic anhydride in the presence of 4-phenylethynylphthalic anhydride as an end-capping agent. The effects of the resin chemical structures and molecular weights on their melt processability and thermal properties were systematically investigated. The experimental results demonstrated that the molecular-weight-controlled imide resins exhibited not only meltability and melt stability but also low melt viscosity and high fluidability at temperatures lower than 280°C. The molecular-weight-controlled imide resins could be thermally cured at 371°C to yield thermoset polyimides by polymer chain extension and crosslinking. The neat thermoset polyimides showed excellent thermal stability, with an initial thermal decomposition temperature of more than 500°C and high glass-transition temperatures greater than 290°C, and good mechanical properties, with flexural strengths in the range of 140.1–163.6 MPa, flexural moduli of 3.0–3.6 GPa, tensile strengths of 60.7–93.8 MPa, and elongations at break as high as 14.7%. © 2007 Wiley Periodicals, Inc. J Appl Polym Sci 107: 755–765, 2008

Key words: mechanical properties; polyimides; thermal properties; viscosity

INTRODUCTION

Aromatic polyimides, because of their excellent thermal, mechanical, electrical-insulation, and dielectric properties, have found widespread applications both in the aerospace/aeronautical industry and in the semiconductor manufacturing and advanced microelectronics packaging industry.[1,2] However, the rigid polymer backbones and the strong polymer chain-to-chain interactions make aromatic polyimide materials infusible and insoluble. Hence, aromatic polyimide films or coatings are usually produced through the casting of polyimide precursors [poly(amic acid)s] followed by thermal curing to complete the imidization of poly(amic acid)s at elevated temperatures (>250°C) with the release of irritating and poisonous organic volatiles. As for the matrix resins of fiber-reinforced composites, low-molecular-weight and reactive end-capped imide resins are employed that can be easily impregnated with carbon (or glass) fibers and melted at an elevated temperature to yield high-flowing molten fluids followed by thermal curing at a high temperature to produce thermoset polyimides by polymer chain extension and crosslinking.[3] However, the thermoset polyimides obtained in this way are brittle, being suited for the fabrication of thick and large composite components. Therefore, finding melt-processable aromatic polyimides with both high thermal properties and high toughness has been a big scientific and technological challenge.

In recent years, it has been found that phenylethynyl-end-capped imide oligomers[4–22] with low molecular weights (5000–9000 g/mol) can be melt-processed at 350–371°C to yield high-toughness polyimides. Moreover, phenylethynyl-end-capped imide oligomers with calculated molecular weights as low as 750 g/mol can be melted at 280°C to produce low-viscosity and stable molten fluids that can be thermally cured at 350–371°C, exhibiting good features for resin transfer molding (RTM) processing. Hence, many efforts have been made recently to develop aromatic polyimide resins for RTM applications. Three phenylethynyl-terminated imide (PETI) oligomers with different glass-transition temperatures (T_g's), named PETI-298, PETI-330, and PETI-375, respectively, have been developed and employed to fabricate carbon fiber/polyimide composite laminates by RTM. The mechanical properties, including the fracture toughness and tensile or flexural strength (or modulus), of the melt-processed polyimides are closely related to their chemical structures, molecular weights, and molecular weight

Correspondence to: S. Y. Yang (shiyang@iccas.ac.cn).

Journal of Applied Polymer Science, Vol. 107, 755–765 (2008)

distributions as well as their thermal-curing parameters and so forth.[23–27] Hence, it is still a big issue to investigate the relationship between the chemical structure of a polyimide and its melt processability as well as the mechanical properties.

In this study, a series of novel molecular-weight-controlled and phenylethynyl-end-capped imide resins based on a fluorinated aromatic diamine, 1,4-bis(4-amino-2-trifluoromethylphenoxy)benzene (1,4,4-6FAPB), were prepared. The effects of the chemical structures and molecular weights of the imide resins on their melt processability as well as the thermal and mechanical properties of the thermally cured polyimides were systematically investigated.

EXPERIMENTAL

Materials

1,4,4-6FAPB and 1,3-bis(4-aminophenoxy)benzene (1,3,4-APB) were synthesized according to the reported method in this laboratory.[28] 4-Phenylethynylphthalic anhydride (PEPA) was prepared according to methods in the literature. 4,4′-Oxydiphthalic anhydride (ODPA; Shanghai Research Institute of Synthetic Resin, Shanghai, China) was purchased and dried in a vacuum oven at 180°C for 12 h before use. *N*-Methyl-2-pyrrolidinone (NMP) was purified by vacuum distillation over P_2O_5 before use. Toluene (Beijing Beihua Fine Chemicals Co., Beijing, China) was used as received without further purification.

Preparation of the phenylethynyl-end-capped imide resins

The phenylethynyl-end-capped imide resins, designed with calculated number-average molecular weights (M_n's) of 1250–10,000 g/mol, were prepared through the reaction of ODPA with a mixture of 1,4,4-6FAPB and 1,3,4-APB in the presence of PEPA as an end-capping agent in NMP at elevated temperatures (Scheme 1). In a typical experiment, PI-1 (ODPA–1,4,4-6FAPB/1,3,4-APB–PEPA) was prepared with the following procedure.

Into a three-necked, 250-mL flask equipped with a mechanical stirrer, thermometer, nitrogen gas inlet/outlet, Dean–Stark trap, and condenser were placed 1,4,4-6FAPB (5.6154 g, 13.11 mmol), 1,3,4-APB (11.4973 g, 39.33 mmol), and NMP (28.0 mL). The mixture was stirred at the ambient temperature for ~ 1 h until the aromatic diamines were completely dissolved to produce a homogeneous solution. Next, a slurry of ODPA (6.9642 g, 22.45 mmol) and PEPA (14.8938 g, 60.00 mmol) in 28.0 mL of NMP was added. An additional 13.0 mL of NMP was used to rinse all the anhydrides, and this resulted in a reaction mixture with ~ 35% solids (w/w). The reaction mixture was stirred in nitrogen at 75°C for 4 h, and 5.0 mL of toluene was then added. The reaction

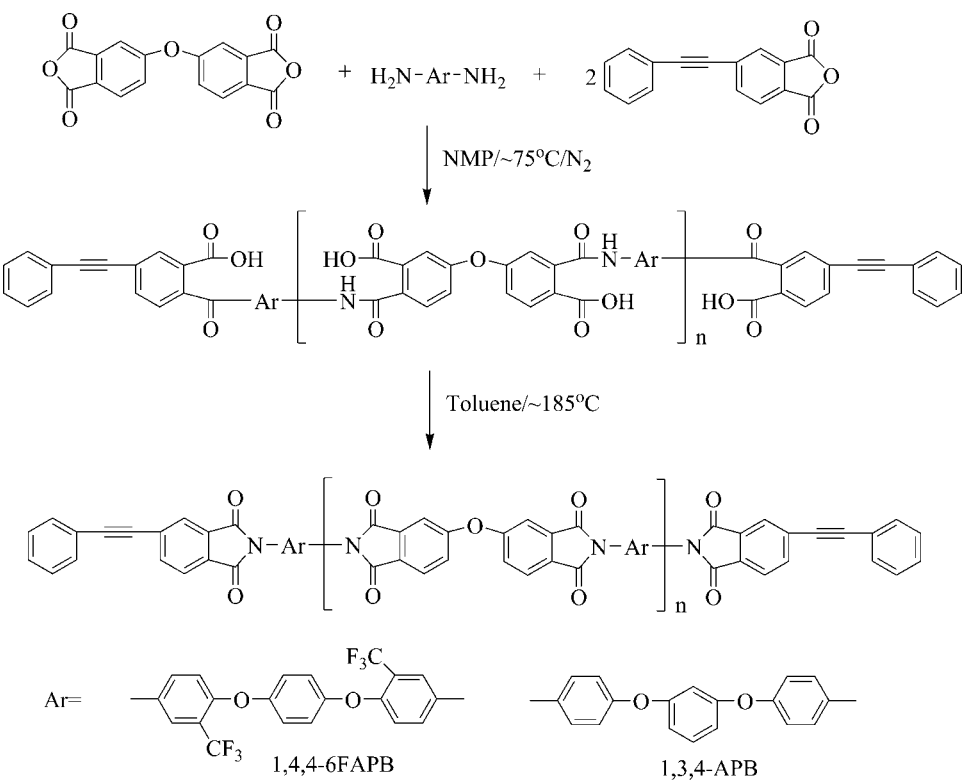

Scheme 1 Synthesis of the phenylethynyl-end-capped imide resins.

TABLE I
Stoichiometry of the Phenylethynyl-End-Capped Imide Resins

Sample	Aromatic diamine (mmol)	ODPA (mmol)	PEPA (mmol)	Calculated molecular weight
PI-1	1,4,4-6FAPB (13.11) 1,3,4-APB (39.33)	22.45	60.00	1,250
PI-2	1,4,4-6FAPB (25.21) 1,3,4-APB (25.21)	20.42	60.00	1,250
PI-3	1,4,4-6FAPB (42.54) 1,3,4-APB (14.18)	21.73	70.00	1,250
PI-4	1,4,4-6FAPB (45.60) 1,3,4-APB (45.60)	66.20	50.00	2,500
PI-5	1,4,4-6FAPB (37.88) 1,3,4-APB (37.88)	65.76	20.00	5,000
PI-6	1,4,4-6FAPB (50.00) 1,3,4-APB (50.00)	93.50	13.00	10,000

solution was gradually heated to 185–205°C, and the water that evolved during the thermal imidization was removed simultaneously by azeotropic distillation. Approximately 8–10 h was required to complete the thermal imidization reaction. After it cooled to ~ 120°C, the reaction solution was poured into an excess of warm water with stirring to precipitate the imide resin. The solid resin was then isolated by filtration, thoroughly washed with warm water, and then dried at 60°C overnight to remove most of the water. Complete drying of the imide resin was performed at 135°C in a vacuum oven for ~ 24 h to yield 36.02 g (97%) of PI-1.

PI-2–PI-6 were synthesized with a similar procedure with designed molar ratios of 1,4,4-6FAPB to 1,3,4-APB and calculated M_n values, as described in Table I.

Thermal curing of the molecular-weight-controlled imide resins

The molecular-weight-controlled imide resin powders were placed in a die, which was then placed in a hot press preheated at 200°C. The die temperature was increased gradually to 371°C at a rate of 4°C/min. After it was kept there for 15–20 min, the die was applied with a pressure of 1.0–3.5 MPa. After it was kept for 1 h at 371°C, the die was then cooled with the applied pressure to less than 200°C. The thermally cured polyimide sheet was removed from the die at room temperature and was then cut to the desired sizes for thermal and mechanical testing.

Characterization and measurements

Differential scanning calorimetry (DSC) was performed on a PerkinElmer 7 series thermal analysis system (Perkin Elmer Corp., Norwalk, CT) in a nitrogen atmosphere at a flow rate of 20 cm^3/min, and the scanning range was 70–420°C. The imide resin powder was heated at a rate of 10°C/min to observe its thermal curing behavior. The thermally cured polyimide was measured at a rate of 20°C/min. T_g was determined as the inflection point of the curve of the heat flow versus the temperature.

Matrix-assisted laser desorption/ionization time-of-flight (MALDI-TOF) mass spectra were obtained with a Biflex III MALDI-TOF mass spectrometer (Bruker, Billerica, Germany) equipped with delayed extraction, a multisample probe, a time-of-flight reflectron analyzer, a nitrogen laser with a wavelength of 337 nm and a pulse width of 3 ns, and a linear flight path length of 100 cm. The flight tube was evacuated to 10^{-7} Pa. All measurements were performed in a reflection mode with positive-ion detection. The acceleration voltage was 19 kV, and the delayed extraction voltage was 14.5–17 kV.

The complex viscosity (η^*) was measured on a TA AR2000 rheometer (TA Instruments Corp., New Castle, DE). An imide resin disk, 25 mm in diameter and ~ 1.5 mm thick, was prepared through the press molding of the molecular-weight-controlled imide resin powder at room temperature, which was then loaded into a rheometer fixture equipped with 25-mm-diameter parallel plates. The top plate was oscillated at a fixed strain of 5% and a fixed angular frequency of 100 rad/s, whereas the lower plate was attached to a transducer, which was used to record the resultant torque. In the temperature ramp procedure, an initial temperature of 200°C was set, and then the parallel plates with the testing sample were equilibrated at this temperature for 10 min. η^* as a function of the scanning temperature was measured by temperature scanning from 200 to 420°C at a rate of 4°C/min. In the time sweep procedure, the parallel plates with the testing sample were equilibrated at 200°C for 10 min. The specimens were heated from 200 to 280°C at a heating rate of 4°C/min and then were held for 2 h at 280°C to assess the melt stability. η^* as a function of the time and temperature was measured.

The inherent viscosities were obtained through the dissolution of the molecular-weight-controlled imide resin powder in NMP at a concentration of 0.5% (w/v) followed by the measurement of the elution time with an Ubbelohde viscometer (Shanghai Liang Jing Glass Instrument Factory, Shanghai, China) in a thermostated 25°C water bath.

Thermogravimetric analysis (TGA) was performed on a PerkinElmer 7 series thermal analysis system at a heating rate of 20°C/min in a nitrogen atmosphere at a flow rate of 20 cm^3/min.

Dynamic mechanical analysis (DMA) was performed on a PerkinElmer 7 series thermal analysis system, and the scanning temperature range was 50–400°C at a heating rate of 5°C/min and at a frequency of 1 Hz. A three-point-bending mode was employed, and the specimen size was 15.0 × 3.0 × 1.2 mm^3. The storage modulus, loss modulus, and tangent of the loss angle (tan δ) were obtained as functions of the scanning temperature.

IR spectra were recorded in the transmission mode with a PerkinElmer 782 Fourier transform infrared (FTIR) spectrophotometer.

Gel permeation chromatography (GPC) measurements were performed with a Waters 1515 high-performance liquid chromatography (HPLC) pump (Waters Corp., Milford, MA) equipped with a Waters 2414 refractive-index detector. A set of three Waters Styragel columns (2 HR0.5 columns and 1 HR1 column), kept at 35 ± 0.1°C, were used with HPLC-grade tetrahydrofuran as the mobile phase at a flow rate of 1.0 mL/min.

Wide-angle X-ray diffraction was conducted on a Rigaku D/max-2500 X-ray diffractometer (Rigaku Corp., Tokyo, Japan) with Cu Ka1 radiation at 40 kV and 200 mA.

Measurements of the mechanical properties were performed with an Instron model 3365 universal tester (Instron Corp., Canton, MA) at room temperature. The tensile strength, modulus, and elongation at break were measured in accordance with GB/T 16421-1996 at a strain rate of 2 mm/min. The flexural strength and flexural modulus were measured in accordance with GB/T 16419-1996 at a span-to-depth ratio of 16 at a rate of 1 mm/min.

RESULTS AND DISCUSSION

Synthesis and characterization of the phenylethynyl-end-capped imide resins

The phenylethynyl-end-capped imide resins, designed with calculated M_n values of 1250, 2500, 5000, and 10,000 g/mol, were prepared with a one-step high-temperature polycondensation procedure (Scheme 1). The aromatic dianhydride (ODPA) and the mixture of aromatic diamines (1,4,4-6FAPB and 1,3,4-APB) in the presence of the end-capping agent were first polycondensed in an NMP solution at 75°C to yield a phenylethynyl-end-capped poly(amic acid) resin, which was then thermally imidized at an elevated temperature to give a phenylethynyl-end-capped imide resin. The water that evolved as a byproduct of the thermal cyclization and imidization was removed simultaneously in the presence of toluene by azeotropic distillation to push the thermal cyclization and imidization to completion. Thus, a series of phenylethynyl-end-capped imide resins with different calculated M_n values and different molar ratios of 1,4,4-6FAPB to 1,3,4-APB were prepared (Table I), including PI-1 (M_n = 1250 g/mol) derived from ODPA, 1,4,4-6FAPB/1,3,4-APB (1:3), and PEPA; PI-2 (M_n = 1250 g/mol) derived from ODPA, 1,4,4-6FAPB/1,3,4-APB (1 : 1), and PEPA; PI-3 (M_n = 1250 g/mol) derived from ODPA, 1,4,4-6FAPB/1,3,4-APB (3 : 1), and PEPA; PI-4 (M_n = 2500 g/mol) derived from ODPA, 1,4,4-6FAPB/1,3,4-APB (1 : 1), and PEPA); PI-5 (M_n = 5000 g/mol) derived from ODPA, 1,4,4-6FAPB/1,3,4-APB (1 : 1), and PEPA; and PI-6 (M_n = 10,000 g/mol) derived from ODPA, 1,4,4-6FAPB/1,3,4-APB (1 : 1), and PEPA. The imide resin powders were purified through the reprecipitation of the imide resin solution in NMP into an excess of water. After being collected, the solid resins were washed thoroughly with water and dried overnight in a vacuum oven.

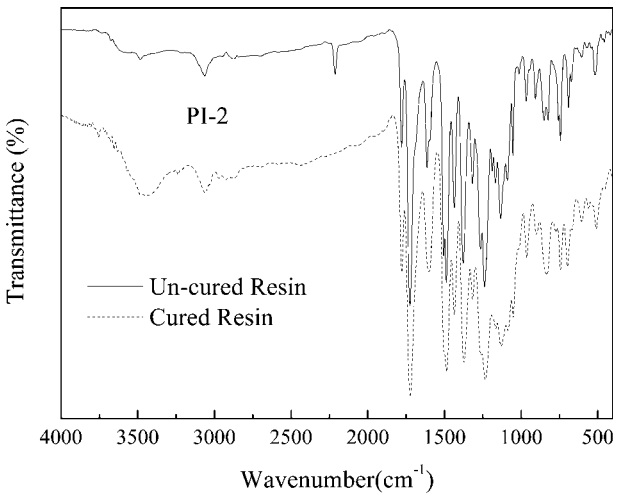

Figure 1 FTIR spectra of the phenylethynyl-end-capped imide resins before and after curing at 371°C for 1 h.

Figure 1 shows typical FTIR spectra of a phenylethynyl-end-capped imide resin (PI-2); asymmetric and symmetric stretching absorptions at 1778 and 1722 cm^{-1}, respectively, assigned to the imide groups in the polymer backbone of the imide resins, can be observed for PI-2. The absorption at 2210 cm^{-1}, assigned to the stretching vibrations of the ethynyl group (—C≡C—) in PI-2, was detected (uncured resin curve in Fig. 1) and then completely

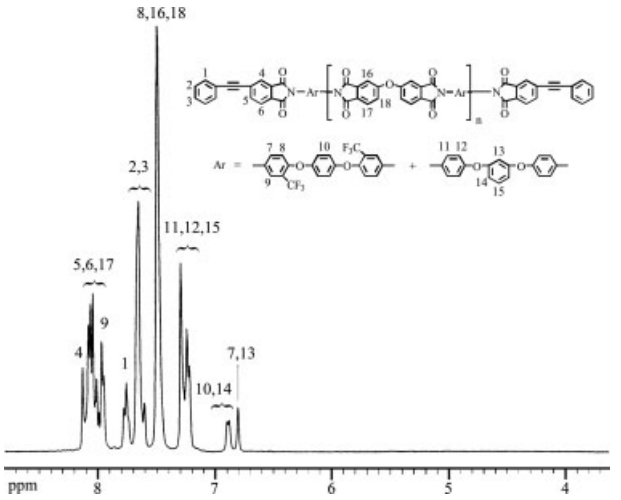

Figure 2 ^{1}H-NMR spectrum of a phenylethynyl-end-capped imide resin (PI-2; DMSO-d_6).

disappeared after the sample was thermally cured at 371°C for 1 h (cured resin curve in Fig. 1), demonstrating that the phenylethynyl groups in PI-2 took part in chemical reactions, most likely polyimide chain extension and crosslinking.

Figure 2 shows the ^{1}H-NMR spectrum of a representative phenylethynyl-end-capped imide resin (PI-2) in dimethyl sulfoxide-d_6 (DMSO-d_6) as a solvent. All the protons in the phenylethynyl-end-capped imide resin, as expected, were detected, and this confirmed that the imide resin had the designed chemical structure.

Table II shows the inherent viscosities and molecular weights of the phenylethynyl-end-capped imide resins, including the calculated M_n, experimental M_n, weight-average molecular weight (M_w), and size-average molecular weight (M_z). The inherent viscosities of the resins were measured in the range of 0.09–0.43 and increased with increases in the calculated molecular weights. For instance, PI-1–PI-3, with a calculated M_n value of 1250, showed an intrinsic viscosity ([η]) of 0.09–0.11, whereas PI-4 had an [η] value of 0.16 (calculated M_n = 2500), and PI-5 had an [η] value of 0.27 (calculated M_n = 5000).

The resin molecular weights also increased with increases in the calculated molecular weights but did not show linear changes. For instance, PI-4 (calculated M_n = 2500) showed M_n = 2093, almost the same as that of PI-2 (2139; calculated M_n = 1250). Figure 3 compares the GPC curves of the phenylethynyl-end-capped imide resins with different designed M_n values of 1250 (PI-2), 2500 (PI-4), and 5000 (PI-5) g/mol. The imide resins contained several molecular weights in a broad elution time range, in which the major molecular weights increased with increases in the calculated M_n value. For instance, PI-5 with a calculated M_n value of 5000 exhibited a major elution time peak at 22.0 min versus 22.5 min for PI-4 (calculated M_n = 2500) and 25.5 min for PI-2 (calculated M_n = 1250). However, the molecular weight distributions obviously changed with increasing molecular weights. In contrast to PI-2, which had five peaks with different relative intensities in the elution time range of 27.5–20.0 min, that is, 26.5 (70%), 25.5 (100%), 23.0 (80%), 22.5 (50%), and 22.3 (40%), PI-4 exhibited six peaks with different relative intensities located at 26.5 (30%), 25.5 (30%), 23.0 (55%), 22.6 (80%), 22.3 (95%), and 22.0 (100%). The peak at 22.0 min (100%) was a new resin species with the highest molecular weight. Moreover, the relative intensities also changed obviously, and the higher molecular weights were greatly intensified. PI-5 showed an intense and broad peak located in the range of 23.0–20.0 min along with traces of other peaks observed for PI-2 and PI-4, and this demonstrated that PI-5 mainly consisted of the high-molecular-weight resin species. Clearly, the molecular weights and molecular weight distributions of the phenylethynyl-end-capped imide resins depended greatly on their designed molecular weights, and high-molecular-weight resin species were easier to form at high calculated values of M_n.

Figure 4 shows the MALDI-TOF mass spectra of the representative phenylethynyl-end-capped imide resins (PI-2 and PI-4); 5 chemical species with molecular weights of 753.2 (776.2 − 23.0 = 753.2), 1319.9 (1342.9 − 23.0), 1456.0 (1479.0 − 23.0), 1887.8 (1910.8 − 23.0), and 2023.9 (2046.9 − 23.0) were detected in PI-2, and more than 12 chemical species with molecular weights in the range of 753.2–3428.0 were observed in PI-4. Table III shows all the expected

TABLE II
Molecular Weights and Inherent Viscosities of the Phenylethynyl-End-Capped Imide Resins

Sample	Calculated M_n (g/mol)	Experimental M_n (g/mol)	M_w (g/mol)	M_z (g/mol)	[η] (dL/g)
PI-1	1,250	1,762	2,797	3,974	0.10
PI-2	1,250	2,139	3,153	4,270	0.09
PI-3	1,250	2,200	3,176	4,204	0.11
PI-4	2,500	2,093	4,408	5,717	0.16
PI-5	5,000	3,234	6,156	7,207	0.27
PI-6	10,000	NA	NA	NA	0.43

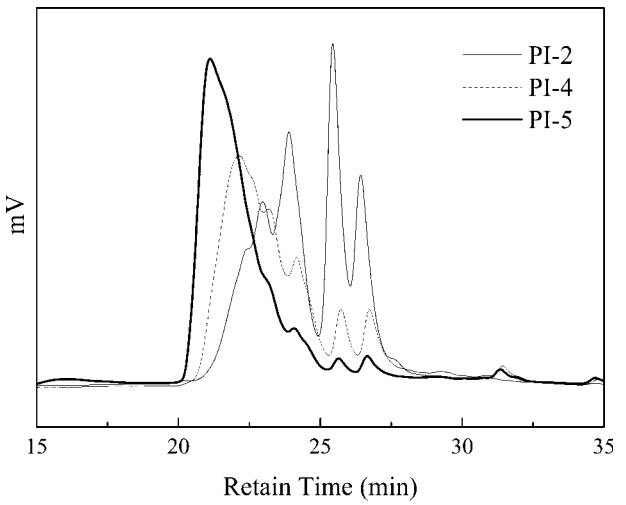

Figure 3 GPC curves of the phenylethynyl-end-capped imide resins.

chemical structures of the imide resins. Clearly, phenylethynyl-end-capped imide resins are chemical oligomer mixtures with different molecular weights, and all the imide oligomer species are biphenylethynyl-end-capped imide resins. Moreover, it seems that 1,3,4-APB is more reactive with PEPA than 1,4,4-6FAPB and yields oligomer PEPA–1,3,4-APB–PEPA (M_n = 753.2). Experimental results indicated that PI-5 (calculated M_n = 5000) contained much higher molecular weight species than PI-4, for which maximum molecular weights as high as 7500–8000 g/mol were detected in MALDI-TOF mass spectra.

Melt processability of the phenylethynyl-end-capped imide resins

Dynamic rheology was employed to investigate the melt processability of the imide resins. The melt rheology was performed with an imide resin disc compressed at room temperature. Table IV shows the complex melt viscosities at different heating temperatures, the minimum melt viscosities, and the melt viscosity variations for 2 h at 280°C for the phenylethynyl-end-capped imide resins. The temperatures at which the imide resin had the minimum melt viscosities were increased from 288°C (0.25 Pa s) for PI-2 (calculated M_n = 1250) to 313°C (6.39 Pa s) for PI-4 (calculated M_n = 2500), 322°C (69.88 Pa s) for PI-5 (calculated M_n = 5000), and 334°C (328.1 Pa s) for PI-6 (calculated M_n = 10,000).

The resin minimum melt viscosities also increased gradually with increases in the calculated M_n values. For instance, PI-2 exhibited a minimum viscosity of 0.25 Pa s at 288°C in contrast to PI-4 (6.39 Pa s at 313°C) and PI-6 (328.1 Pa s at 334°C).

Table IV shows the data for the complex melt viscosities at different temperatures (250, 275, 300, 325, and 350°C) for all of the synthesized imide resins (PI-1–PI-6), and Figure 5 compares the dynamic thermal rheological curves of a series of imide resins with different calculated M_n values, including PI-2, PI-4, PI-5, and PI-6. PI-2 could completely melt at a temperature as low as 250°C [melting temperature (T_m)] and start to rapidly cure at 350°C [curing temperature (T_c)]; hence, the melting temperature width (Δ) was 100°C (250 to 350°C), in contrast to PI-4 (T_m = 300°C, T_c = 340°C, Δ = 40°C), PI-5 (T_m = 310°C, T_c = 330°C, Δ = 20°C), and PI-6 (T_m = 325°C, T_c = 335°C, Δ = 10°C). Meanwhile, the melt viscosity at 325°C for PI-2 was 0.36 Pa s versus 7.18 Pa s for PI-4, 70.18 Pa s for PI-5, and 392.6 Pa s for PI-6. Obviously, the resin meltability and melt processability deteriorated with increases in the calculated M_n values.

The isothermal melt stabilities are also shown in Table IV, and two representative curves of the melt viscosity against the isothermal standing time at 280°C are depicted in Figure 6. The melt viscosity variations at 280 or 290°C for 2 h of standing (Table IV) depend on the calculated M_n values as well as the polymer chemical structures. PI-2 exhibited a

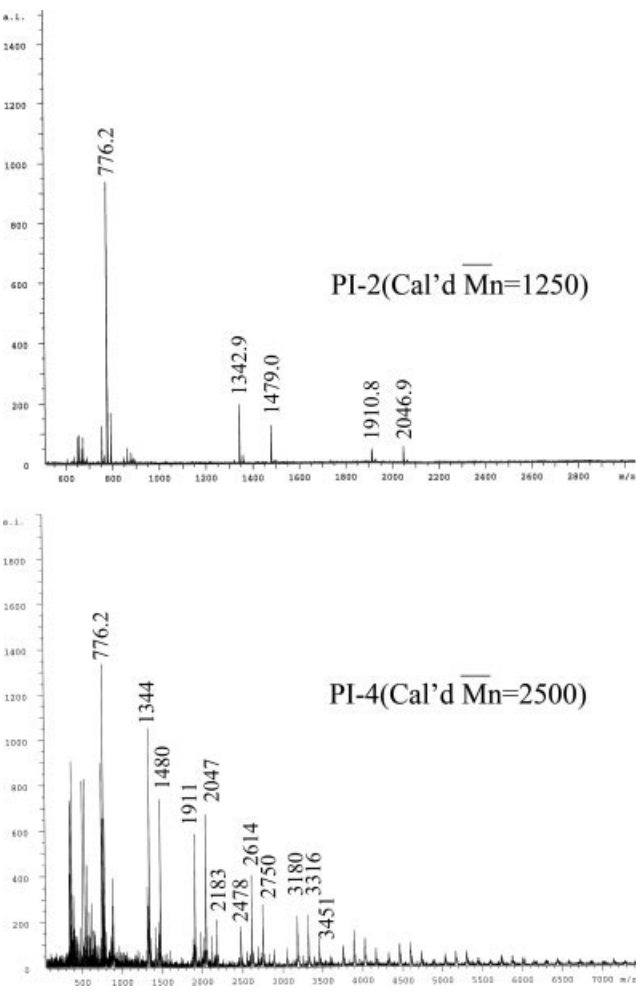

Figure 4 MALDI-TOF mass spectra of the phenylethynyl-end-capped imide resins with calculated molecular weights of 1250 (PI-2) and 2500 (PI-4) g/mol.

TABLE III
Chemical Structure Assignments for the MALDI-TOF Mass Spectra of PI-2 (Calculated M_n = 1250) and PI-4 (Calculated M_n = 2500)

Sample	Chemical structure of the resin species	m/z
PI-2	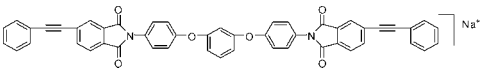	776.2
	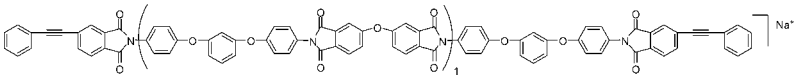	1342.9
	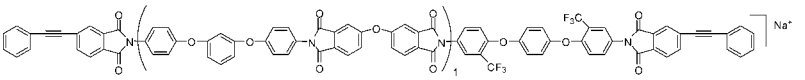	1479.0
	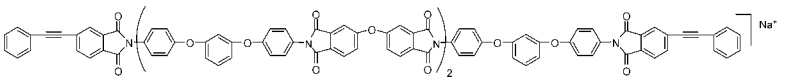	1910.8
	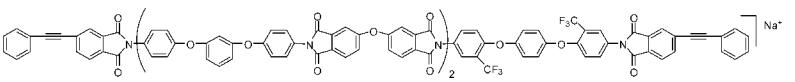	2046.9
PI-4	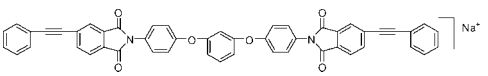	776.2
	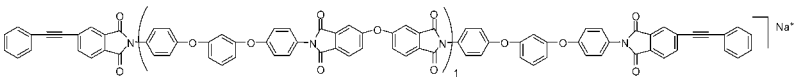	1344
	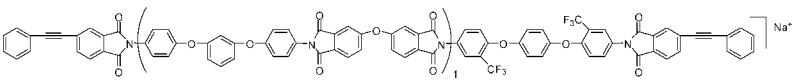	1480
	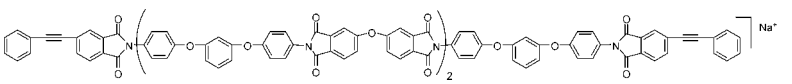	1911
	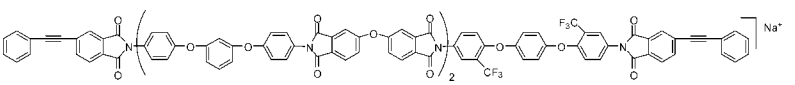	2047
	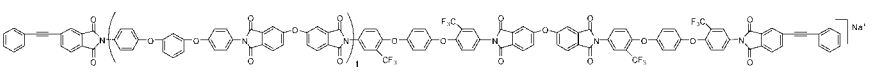	2183
	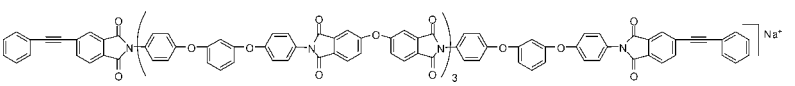	2478
	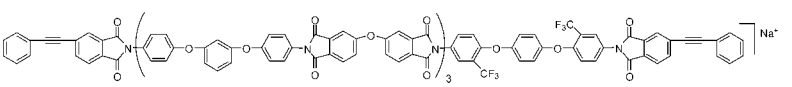	2614
	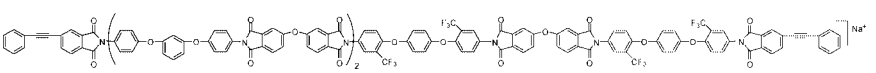	2750
	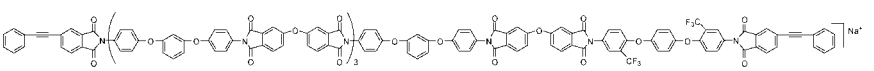	3180
	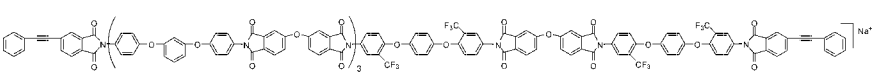	3316
	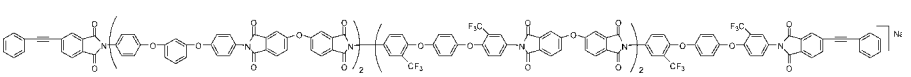	3451

TABLE IV
Complex Melt Viscosity of the Phenylethynyl-End-Capped Imide Resins

Sample	Complex melt viscosity (Pa s) 250°C	275°C	300°C	325°C	350°C	Minimum melt viscosity (Pa s/°C)	Melt viscosity variation at 280°C for 2 h (Pa s)
PI-1	54.1	0.60	0.50	0.57	0.69	0.50 at 300°C	0.57–4.01
PI-2	0.58	0.32	0.31	0.36	0.44	0.25 at 288°C	0.38–0.95
PI-3	0.61	0.36	0.30	0.33	1.78	0.28 at 308°C	0.48–3.30
PI-4	63.31	15.37	7.17	7.18	29.61	6.39 at 313°C	11.56–81.79
PI-5	3801	491.8	121.3	70.48	1162	69.88 at 322°C	264.8–1563[a]
PI-6	27,010	8,349	1,389	392.6	418.8	328.1 at 334°C	896.4–5378[b]

[a] Melt viscosity variation at 290°C for 2 h.
[b] Melt viscosity variation at 310°C for 2 h.

melt viscosity variation at 280°C of 0.38–0.95 Pa s (Fig. 6), in contrast to PI-4 (11.5–81.79 Pa s), and this implied that the melt stabilities of the phenylethynyl-end-capped imide resins were closely related to their molecular weights and distributions as well as the chemical structures.

In addition, the imide resins with the same calculated M_n value but different chemical structures (PI-1, PI-2, and PI-3) also showed different melt stabilities. PI-2 showed the lowest minimum viscosity at 288°C and good melt stability at an elevated temperature.

Figure 7 shows DSC curves of representative phenylethynyl-end-capped imide resins, and Table V summarizes the T_g data obtained from DSC and the data regarding the exothermal absorption peaks, including the onset temperature, the peak temperature, and the end-point temperature. PI-2 exhibits an endothermal absorption peak located at 124°C and assigned to T_g, and a broad and intense exothermal absorption attributed to the thermal curing of the phenylethynyl groups was observed; this implied that the thermal curing of the imide resin was accompanied by a lot of heat release. The T_g values were measured in the range of 124–183°C and increased with increases in the calculated M_n values. For instance, PI-2 showed a T_g value of 124°C versus 161°C for PI-4, 187°C for PI-5, and 183°C for PI-6. This could be interpreted by the changes in the polymer chain lengths. The imide resins were mixtures containing several resin species with different chemical backbones and different chain lengths. The imide resins with higher calculated M_n values contained much higher molecular weight species, and this resulted in the higher T_g values.

In addition, all the exothermal absorptions were measured in the same range, with the onset temperature of 339–344°C, the peak temperature of 383–387°C, and the end-point temperature of 429–432°C. However, the exothermal absorption intensities decreased with increases in the calculated M_n values (Fig. 7). For instance, PI-5 and PI-6, because of their higher calculated M_n values, did not show exothermal absorptions as PI-2 and PI-4 did, probably because of the low concentrations of the end-capping groups in the imide resins.

Thermal properties of the thermoset polyimides

Figure 8 depicts DSC curves of the thermoset polyimides. In comparison with the imide resins (Fig. 7), the exothermal absorption peaks disappeared, and

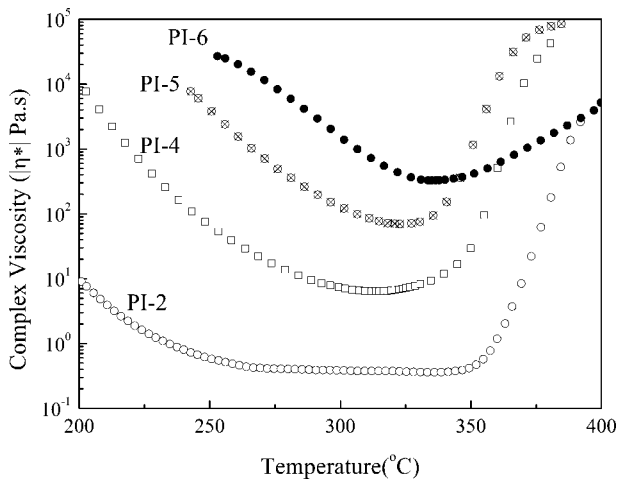

Figure 5 Melt viscosity of the phenylethynyl-end-capped imide resins with different molecular weights.

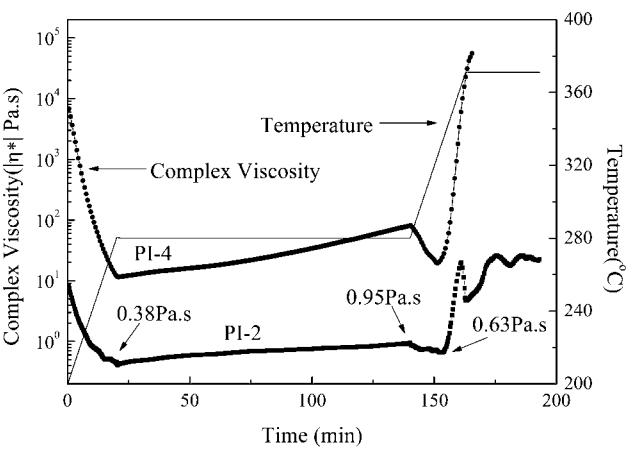

Figure 6 Isothermal melt viscosity at 280°C of typical phenylethynyl-end-capped imide resins (PI-2 and PI-4).

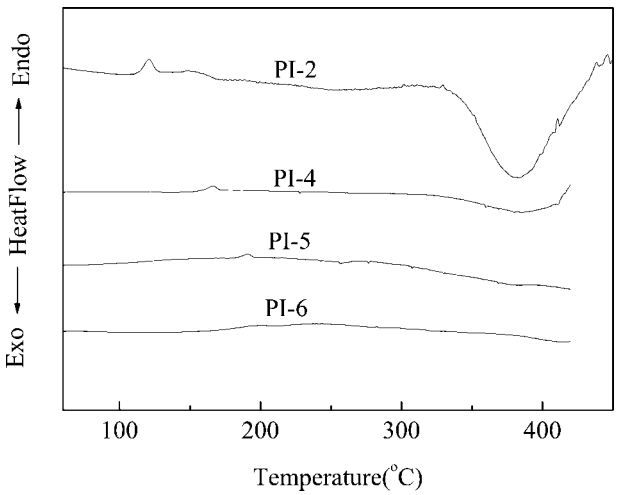

Figure 7 DSC curves of the phenylethynyl-end-capped imide resins.

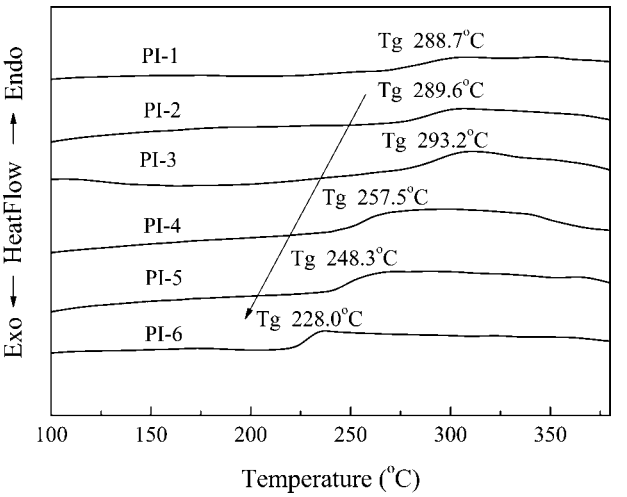

Figure 8 DSC curves of the thermoset polyimides cured at 371°C for 1 h.

this demonstrated that all the phenylethynyl groups were completely consumed in the crosslinking and polymer chain extension reactions to yield high-molecular-weight resin species. The T_g values of the thermally cured polyimides were changed with both the polymer chemical backbones and the calculated molecular weights. The T_g value of the thermally cured polyimide increased with decreases in the calculated M_n values, and this resulted from the high polymer chain crosslinking density. PI-2 exhibited a T_g value of 289.6°C, which was 32.1°C higher than that of PI-4 and 61.6°C higher than that of PI-6 (228.0°C). In addition, PI-1, for which the molar ratio of 1,4,4-6FAPB to 1,3,4-APB was 1 : 3, had a T_g value of 288°C, only 5°C lower than that of PI-3 (1,4,4-6FAPB/1,3,4-APB = 3 : 1).

Figure 9 shows DMA curves of a representative thermoset polyimide (PI-2), and Table VI summarizes the DMA data for all the thermally cured polyimides (PI-1–PI-6), including the storage modulus, loss modulus, and tan δ. The thermoset polyimides showed T_g values in the range of 224–341°C, which decreased with increases in the calculated M_n values. For instance, PI-2 (calculated M_n = 1250) showed a T_g value of 317°C, 93°C higher than that of PI-6 (calculated M_n = 10,000). The storage modulus did not decrease until the temperature was scanned to 275°C, and this implied that the thermally cured polyimide had outstanding thermomechanical properties.

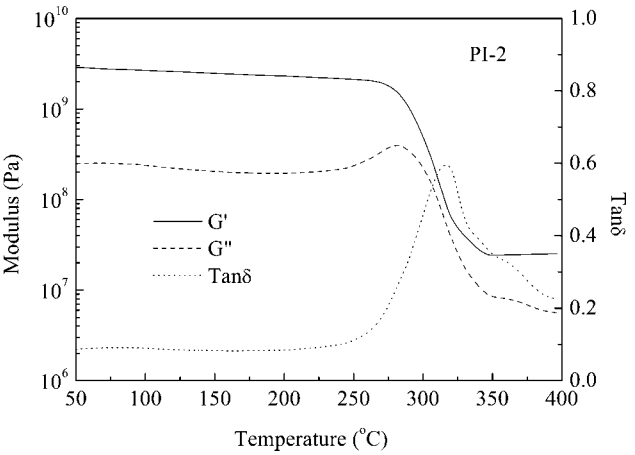

Figure 9 DMA curves of the thermoset polyimide (PI-2) cured at 371°C for 1 h (G' is the storage modulus, and G'' is the loss modulus).

TABLE V
DSC Data for the Phenylethynyl-End-Capped Imide Resins

Sample	T_g (°C)[a]	Exothermal absorption		
		Onset (°C)	Peak (°C)	End point (°C)
PI-1	126	339	383	432
PI-2	124	339	386	429
PI-3	124	341	386	431
PI-4	161	344	387	432
PI-5	187	—[b]	—[b]	—[b]
PI-6	183	—[b]	—[b]	—[b]

[a] The T_g data were measured at a rate of 10°C/min.
[b] Exothermal absorption was not detected.

TABLE VI
DMA Data for the Thermoset Polyimides Cured at 371°C for 1 h

Sample	G' (°C)[a]	G'' (°C)[b]	Tan δ (°C)[c]
PI-1	280	292	327
PI-2	273	282	317
PI-3	291	308	341
PI-4	235	245	273
PI-5	225	232	251
PI-6	202	208	224

[a] Onset temperature in the storage modulus curve.
[b] Peak temperature in the loss modulus curve.
[c] Peak temperature in the tan δ curve.

TABLE VII
Thermal Properties of the Thermoset Polyimides Cured at 371°C for 1 h

Sample	T_d (°C)	T_5 (°C)	T_{10} (°C)	Char at 700°C (%)
PI-1	571	557	602	69.0
PI-2	574	547	597	67.5
PI-3	589	576	616	71.3
PI-4	591	582	615	69.9
PI-5	595	593	620	69.4
PI-6	602	600	627	69.2

The phenylethynyl-end-capped imide resins could be thermally cured at 371°C for 1 h to produce thermoset polyimides. Table VII summarizes the thermal properties of the thermoset polyimides, including the initial thermal decomposition temperature (T_d), the temperature at a 5% loss of the original weight (T_5), the temperature at a 10% loss of the original weight (T_{10}), and the char yield at 700°C, and it can be seen that the thermoset polyimides showed excellent thermal properties. For instance, the thermoset PI-2 had a T_d value of 574°C, a T_5 value of 547°C, and a T_{10} value of 597°C. In addition, the thermal stabilities of the thermoset polyimides were improved, to some extent, with increases in the calculated M_n values. Figure 10 compares the TGA curves of a series of thermoset polyimides with different calculated M_n values, including PI-2, PI-4, PI-5, and PI-6; no obvious weight loss was detected before the temperature was scanned up to 450°C, and this demonstrated excellent thermal stability.

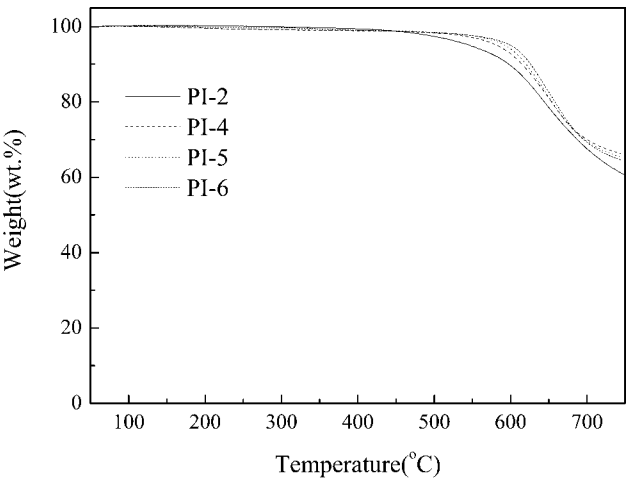

Figure 10 TGA curves of the thermoset polyimides cured at 371°C for 1 h.

Mechanical properties of the thermally cured polyimides

Table VIII summarizes the mechanical properties of the thermoset polyimides. After being thermally cured at 371°C for 1 h, all the thermoset polyimide sheets exhibited excellent mechanical properties, with tensile strengths of 60.7–93.8 MPa, tensile moduli of 1.1–1.7 GPa, elongations at break of 4.3–14.7%, flexural strengths of 140.1–163.6 MPa, and flexural moduli of 3.0–3.6 GPa. The tensile strengths and elongations at break apparently improved gradually with increases in the calculated M_n values from 1250 to 5000. No more benefit for improving the mechanical properties was observed when the calculated M_n values was over 5000. The lower tensile strength and elongation at break of PI-2 and PI-4 versus those of PI-5 were probably due to the higher concentrations of low-molecular-weight resin species in the imide resins. PI-5 exhibited the best mechanical properties, with a tensile strength of 93.8 MPa, an elongation at break of 14.7%, a flexural strength of 140.1 MPa, and a flexural modulus of 3.1 GPa.

In addition, X-ray diffraction patterns of the thermoset polyimides demonstrated that the thermoset polyimides did not contain any crystalline-like phase; they were amorphous polymer materials with low water uptakes in the range of 0.68–0.85%.

CONCLUSIONS

A series of molecular-weight-controlled and phenylethynyl-end-capped imide resins were prepared, and the molecular weights and molecular weight distributions as well as the polymer chemical structures had dramatic effects on their meltability and melt stability. The typical phenylethynyl-end-capped imide resin could be completely melted at temperatures as low as 250–260°C to give a very stable imide resin melt, which could be thermally cured at 371°C to yield a thermoset polyimide by polymer chain extension and crosslinking. The thermoset polyimides showed excellent thermal stability, with T_d's greater than 500°C

TABLE VIII
Mechanical Properties of the Thermally Cured Polyimide Sheets

Sample	Tensile strength (MPa)	Tensile modulus (GPa)	Elongation at break (%)	Flexural strength (MPa)	Flexural modulus (GPa)	Water uptake (wt %)
PI-2	60.7	1.7	4.3	163.6	3.0	0.75
PI-4	68.8	1.1	8.4	147.3	3.3	0.85
PI-5	93.8	1.2	14.7	140.1	3.1	0.76
PI-6	88.0	1.1	12.1	154.1	3.6	0.68

and T_g's of 220–290°C, and good mechanical properties, with flexural strengths that could be higher than 140 MPa and flexural moduli greater than 3.0 GPa.

References

1. Polyimides; Wilson, D.; Stenzenberger, H. D.; Hergenrother, P. M., Eds.; Blackie: Glasgow, 1990.
2. Sroog, C. E. Prog Polym Sci 1991, 16, 561.
3. Serafini, T. T.; Delvigs, P.; Lightsey, G. R. J Appl Polym Sci 1972, 16, 905.
4. Harris, F. W.; Padaki, S. M.; Vavaprath, S. Polym Prepr 1980, 3, 213.
5. Harris, F. W.; Pamidimukkala, A.; Gupta, R.; Das, S.; Wu, T.; Mock, G. J Macromol Sci Chem 1984, 21, 1117.
6. Jensen, B. J.; Hergenrother, P. M.; Nwokogu, G. Polymer 1993, 34, 630.
7. Hergenrother, P. M.; Smith, J. G. Polymer 1994, 35, 4857.
8. Johnston, J. A.; Li, F. L.; Harris, F. W.; Takekoshi, T. Polymer 1994, 35, 4865.
9. Takekoshi, T.; Terry, J. M. Polymer 1994, 35, 4874.
10. Hinkley, J. A.; Jensen, B. J. High Perform Polym 1996, 8, 599.
11. Bryant, R. G.; Jensen, B. J.; Hergenrother, P. M. J Appl Polym Sci 1994, 59, 1249.
12. Connell, J. W.; Smith, J. G.; Hergenrother, P. M. High Perform Polym 1997, 9, 309.
13. Smith, J. G.; Connell, J. W.; Hergenrother, P. M. Polymer 1997, 38, 4657.
14. Fang, X. M.; Scola, D. A. J Polym Sci Part A: Polym Chem 1999, 37, 4616.
15. Donghwan, C.; Lawrence, T. D. J Appl Polym Sci 2000, 75, 1278.
16. Donghwan, C.; Lawrence, T. D. J Appl Polym Sci 2000, 76, 190.
17. Roberts, C. C.; Apple, T. M.; Wnek, G. E. J Polym Sci Part A: Polym Chem 2000, 38, 3486.
18. Smith, J. G.; Connell, J. W.; Hergenrother, P. M. J Compos Mater 2000, 34, 615.
19. Smith, J. G.; Belvin, H. L.; Siochi, E. J.; Cano, R. J.; Johnston, N. J. High Perform Polym 2002, 14, 209.
20. Simona, C. D.; Scola, D. A. Macromolecules 2003, 36, 6780.
21. Liu, H. B.; Simone, C. D.; Scola, D. A. J Polym Sci Part A: Polym Chem 2003, 41, 2630.
22. Zhou, H. W.; Chen, C. H.; Kanbara, R.; Sasaki, T.; Yokota, R. High Perform Polym 2005, 17, 193.
23. Criss, J. M.; Arendt, C. P.; Connell, J. W.; Smith, J. G.; Hergenrother, P. M. SAMPE J 2000, 36, 32.
24. Smith, J. G.; Connell, J. W.; Hergenrother, P. M. J Compos Mater 2002, 36, 2255.
25. Smith, J. G.; Connell, J. W.; Hergenrother, P. M.; Ford, L. A.; Criss, J. M. Macromol Symp 2003, 199, 401.
26. Connell, J. W.; Smith, J. G.; Hergenrother, P. M.; Criss, J. M. High Perform Polym 2003, 15, 375.
27. Smith, J. G.; Connell, J. W.; Li, C. J.; Wu, W.; Criss, J. M. High Perform Polym 2006, 18, 341.
28. Xie, K.; Zhang, S. Y.; Liu, J. G.; He, M. H.; Yang, S. Y. J Polym Sci Part A: Polym Chem 2001, 39, 2581.